Fullerene Complexes

DOI: 10.1002/anie.200604327

Concave Tetrathiafulvalene-Type Donors as Supramolecular Partners for Fullerenes**

Emilio M. Pérez, María Sierra, Luis Sánchez, M. Rosario Torres, Rafael Viruela, Pedro M. Viruela, Enrique Ortí, and Nazario Martín**

The self-assembly of judiciously designed molecular components, based on the dynamic nature of noncovalent interactions, has already allowed the construction of structurally well-defined nanostructures.[1] With the long-term goal of constructing self-assembled nanosized optoelectronic devices, we embarked on the design and synthesis of a suitable donor–acceptor pair. Fullerenes are our electron-acceptor fragment of choice, as their well-known photophysical and electrochemical properties have already been exploited in a wide range of functional chemical species.[2] In particular, noncovalent nanostructures, such as "onions",[3] "peapods",[4] polymeric networks,[5] and dendrimers,[6] have been successfully constructed using aromatic π–π-stacking interactions between the surface of fullerenes and different kinds of receptors.[7] With regards to the electron-donor fragment, the ideal partner for fullerenes should 1) show good electron-donor properties, 2) absorb light efficiently, preferably in the visible region, and 3) self-assemble with fullerenes in a controlled fashion.

Following the seminal work with tetrathiafulvalene (TTF), a rich toolbox of molecules decorated with 1,3-dithiole moieties have been studied as electron donors in photoinduced electron-transfer processes involving fullerenes as acceptors.[8] Among these, π-extended TTF derivatives[9]—in which the dithioles are connected to a π-conjugated core—have been shown to exhibit improved photophysical properties.[10] Furthermore, the concave aromatic surface of 2-[9-(1,3-dithiol-2-ylidene)anthracen-10(9*H*)-ylidene]-1,3-dithiole (exTTF) has been successfully exploited in the molecular recognition of C_{60}.[11] For our purposes, we noticed that a truxene core[12] would be particularly well suited as a scaffold, as its extended π-delocalized system should result in a significant shift of the electronic absorption spectrum towards the visible region and at the same time provide a large aromatic surface with which fullerenes might establish favorable noncovalent interactions. With this in mind, we designed truxene-TTFs **3** which feature three dithiole units connected to a truxene core.

Truxene-TTFs **3a–c** were synthesized starting from commercially available truxenone **1** (Scheme 1). A threefold Wittig–Horner olefination reaction of **1** with the carbanion generated in situ from the corresponding phosphonate esters (**2a–c**)[13] in the presence of *n*BuLi led to the target TTF derivatives **3a–c** in 42–67% yields.

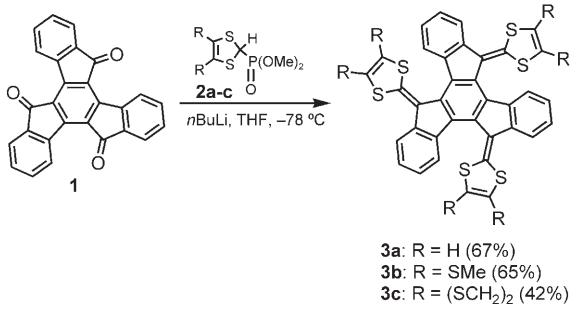

Scheme 1. Synthesis of the truxene-TTF derivatives **3a–c**.

Single crystals suitable for X-ray diffraction were obtained by slow diffusion of cyclohexane vapor into a solution of **3a** in chloroform (Figure 1).[14] To accommodate the dithioles, the truxene moiety breaks down its planar structure and adopts an all-*cis* spherelike geometry with the three dithiole rings protruding outside. This arrangement results in the generation of a molecule with threefold helical chirality of which only the *P*,*P*,*P*/*M*,*M*,*M* enantiomeric pair can be found in the crystal structure. Starting from a hypothetically planar structure for **3a**, these two enantiomers can be easily generated by folding the dithiole rings up or

[*] Dr. R. Viruela, Dr. P. M. Viruela, Dr. E. Ortí
Institut de Ciència Molecular
Universitat de València
46980 Paterna (Spain)
Fax: (+34) 96-354-3274
E-mail: enrique.orti@uv.es
Dr. E. M. Pérez, M. Sierra, Dr. L. Sánchez, Prof. Dr. N. Martín
Departamento de Química Orgánica
Facultad de C. C. Químicas
Universidad Complutense de Madrid
28040 Madrid (Spain)
Fax: (+34) 91-394-4103
E-mail: nazmar@quim.ucm.es
Dr. M. R. Torres
Laboratorio de Difracción de Rayos X
Facultad de C. C. Químicas
Universidad Complutense de Madrid
28040 Madrid (Spain)

[**] This work was supported by the Ministerio de Educación y Ciencia (MEC) of Spain through projects CTQ2005-02609/BQU, BQU2003-05111, and CTQ2004-03760/BQU, and by the Comunidad de Madrid (grant P-PPQ-000225-0505). European FEDER funds (grant BQU2003-05111) are also acknowledged. M.S. and E.M.P. are indebted to MCyT and MEC for a research grant and a Juan de la Cierva postdoctoral contract, respectively. We thank Dr. M. A. Herranz for helpful discussions and Dr. C. Raposo (Universidad de Salamanca) for generously providing the software for binding constant analysis.

Supporting information for this article is available on the WWW under http://www.angewandte.org or from the author.

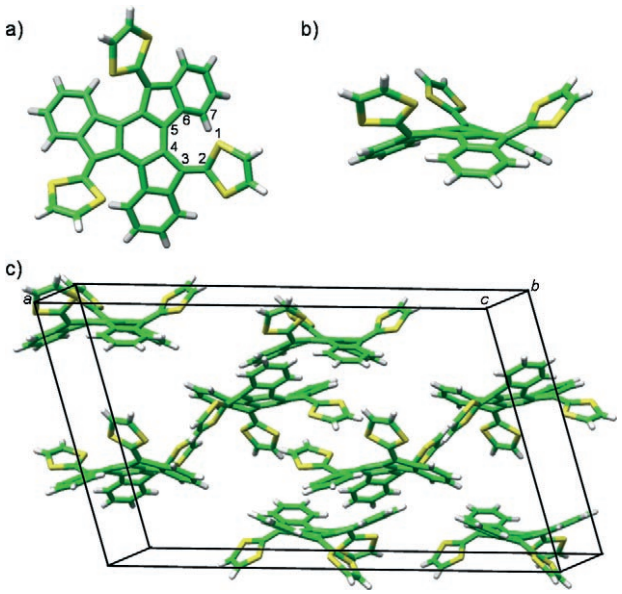

Figure 1. X-ray crystal structure of **3a**:[14] a) (*P,P,P*)-**3a** (top view); b) (*P,P,P*)-**3a** (side view); and c) unit cell showing the racemic mixture. Solvent molecules have been removed for clarity. S yellow, C green, H white.

down. Interestingly, each enantiomer appears, forming homochiral dimers in the unit cell (Figure 1c). The concave bowl-shaped configuration adopted by the truxene core perfectly mirrors the convex surface of fullerenes, suggesting that van der Waals and concave–convex π–π interactions[7] between them should be maximized.

The molecular structure and electronic properties of compound **3a** were theoretically investigated at the B3LYP/6-31G** level (see the Supporting Information). Pristine truxene and 9-(1,3-dithiol-2-ylidene)fluorene[15] (**4**; see Figure 2) were studied as reference systems. The minimum-energy conformation calculated for **3a** corresponds to a C_3-symmetric structure with the symmetry axis passing through the center of the inner benzene ring (see Figure S1 in the Supporting Information). The predicted structure is in agreement with the X-ray crystal structure depicted in Figure 1. To avoid the steric interactions between the dithioles and the peripheral benzene rings, **3a** twists around the C3–C4 and C4–C5 bonds by 40.3° (C2-C3-C4-C5) and 17.4° (C3-C4-C5-C6), respectively (see Figure 1a for atom-numbering scheme). In the crystal, the average values for these angles are 43.3° and 15.4°, respectively. A small twisting is also observed around the C2–C3 double bond (S1-C2-C3-C4: −1.6° (theoretical), −3.4° (X-ray)). As a result of these twistings, the dithiole rings move away from the benzene rings and the S1 atoms lie at 2.87 Å (av. 2.76 Å (X-ray)) from the H7 atoms.

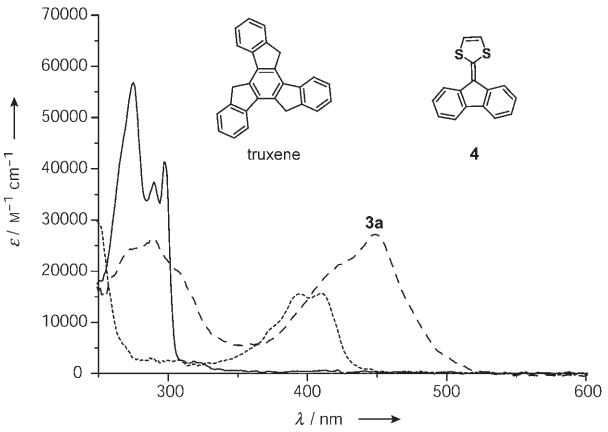

Figure 2. UV/Vis absorption spectra ($CHCl_3$, 298 K) of truxene (——), **4** (••••), and **3a** (-----). The chemical structures of truxene and compound **4** are also shown.

The UV/Vis spectra recorded in $CHCl_3$ for donors **3** (see Figure 2 for **3a**) show the expected bathochromic shift of the lowest-energy absorption band in comparison with the related compound **4**. This shift suggests a higher degree of conjugation in truxene-TTFs **3** despite the loss of planarity. The band is assigned to intramolecular charge transfer from the 1,3-dithiole donor units to the truxene core on the basis of time-dependent density functional theory (TD-DFT) calculations (see the Supporting Information).

The redox behavior of truxene-TTFs **3a–c** was investigated by cyclic voltammetry (CV) in CH_2Cl_2 at room temperature (see Figure 3 for **3a**). Compared with the electron-acceptor truxenone molecule **1**, which shows three reduction waves ($E^1_{red} = -1.15$ V, $E^2_{red} = -1.60$ V, $E^3_{red} = -2.11$ V), the redox behavior measured for the electron donor **3a** is significantly more complex. In a first voltammogram registered up to 1.5 V (Figure 3a), as many as five oxidation processes were observed. When the oxidative scan was limited to 0.95 V (Figure 3b), the cyclic voltammogram showed three oxidation waves, two of which reveal a quasi-reversible character (Figure 3c), which could be in a first approach assigned to the oxidation of the 1,3-dithiole rings. The additional irreversible processes observed in the oxidative scan up to 1.5 V should be therefore associated with the oxidation of the central aromatic skeleton. However, these oxidation processes take place at potential values (1.04 and 1.23 V) that are even lower than those measured for the

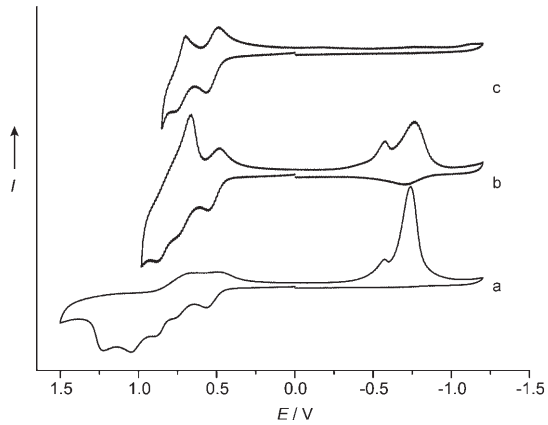

Figure 3. Cyclic voltammograms of compound **3a** in CH_2Cl_2 at 100 mV s^{-1} measured at different oxidative scans: a) from −1.25 to 1.50 V, b) from −1.25 to 0.95 V, and c) from −1.25 to 0.80 V.

truxene molecule (1.36 and 1.61 V) under the same experimental conditions. This observation suggests some cooperative effect between the three 1,3-dithiole rings and the conjugated truxene core. The effect is also observed for the first oxidation potential of compounds **3** (0.56–0.61 V), which is cathodically shifted in comparison with the reference compound **4** (0.71 V). The cyclic voltammogram of **3a** also exhibits intense waves around −0.75 V which seem to be related with reductive desorption processes from the electrode surface.[16]

The substitution of hydrogen atoms in the 1,3-dithiole units of compounds **3b** (R = SMe) and **3c** (R = $(SCH_2)_2$) results in an anodic shift of the oxidation potentials (see Table S1 in the Supporting Information). This effect has been previously reported for related structures[17] and leads to the formation of two broad waves, each one grouping two one-electron oxidation processes.

Table 1 summarizes the charge distribution calculated for the different oxidation states of **3a** using the natural population analysis (NPA) approach. The NPA values indicate that charge in the different steps of the oxidation process is extracted from both the dithiole and the truxene moieties. For $\mathbf{3a}^{3+}$, each dithiole ring has a charge of +0.73e and the truxene core supports a charge of +0.81e. At the end of the oxidation process, that is, for $\mathbf{3a}^{5+}$, three electrons have been extracted from the dithiole rings and the other two electrons have been removed from the truxene backbone. The spin densities calculated for $\mathbf{3a}^{5+}$ indicate that the unpaired electron mainly resides on the C3 atoms (0.25e each) of the truxene moiety. The species $\mathbf{3a}^{5+}$ can be therefore visualized as a truxene radical dication substituted by three aromatic dithiolium cations (6π electrons).

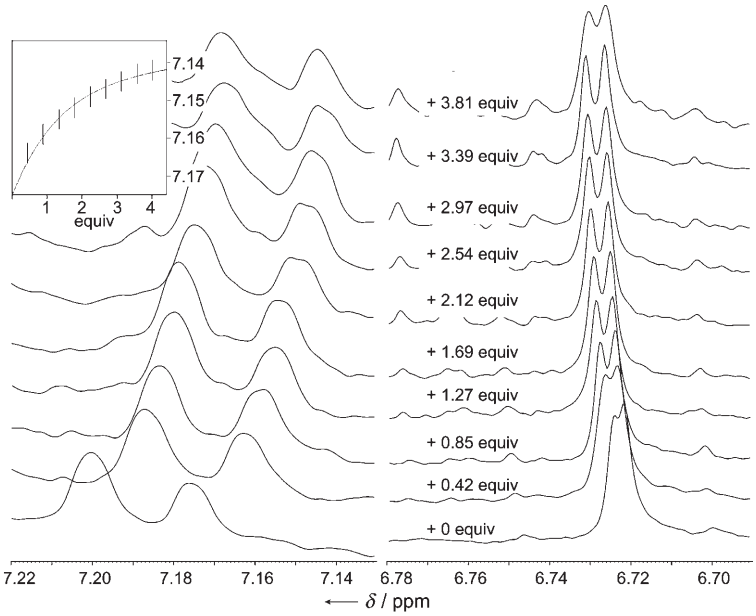

Figure 4. Partial ^{1}H NMR spectra (300 MHz, 298 K, $CDCl_3/CS_2$) of **3a** upon addition of C_{60} depicting the shielding of the aromatic protons (left). Fitting of the chemical shifts to a 1:1 binding isotherm (inset, top left) afforded a binding constant of $(1.2\pm0.3)\times10^3\,M^{-1}$. The slight deshielding of the 1,3-dithiole signals is also shown (right). Similar shifts were observed upon addition of C_{70}, and a binding constant of $(8.0\pm1.5)\times10^3\,M^{-1}$ was calculated.

Table 1: B3LYP/6-31G** NPA charges [e] accumulated by the dithiole rings and the truxene core in the different oxidation states of **3a**.

	3a	$\mathbf{3a}^+$	$\mathbf{3a}^{2+}$	$\mathbf{3a}^{3+}$	$\mathbf{3a}^{4+}$	$\mathbf{3a}^{5+}$
dithiole ring	+0.18	+0.36	+0.54	+0.73	+0.88	+1.00
truxene core	−0.54	−0.08	+0.38	+0.81	+1.36	+2.00

The association of **3a** and fullerenes in solution was investigated by ^{1}H NMR titrations (300 MHz, 298 K) of **3a** (1.18×10^{-3} M, $CDCl_3/CS_2$ 1:1) as host with C_{60} (5.00×10^{-3} M, CS_2) and C_{70} (4.55×10^{-3} M, CS_2) as guests. The progressive shielding (Figure 4, left) of the aromatic protons of **3a** upon addition of the fullerene guests fitted well to a 1:1 binding isotherm[18] and afforded binding constants of $(1.2\pm0.3)\times10^3\,M^{-1}$ and $(8.0\pm1.5)\times10^3\,M^{-1}$ for C_{60} and C_{70}, respectively. A slight deshielding of the dithiole signals (Figure 4, right) owing to charge-transfer interactions between the electron-rich guest **3a** and the electron-poor fullerenes was also observed, suggesting that binding occurs preferentially on the aromatic face of **3a**.

To visualize the association of **3a** with C_{60} and C_{70}, the interaction of these systems was theoretically investigated. Calculations were performed at the DFT level using the MPWB1K density functional, which was recently applied by Truhlar et al.[19] to describe π–π-stacking interactions in stacked DNA base pairs and amino acid pairs.[20]

Fullerene C_{60} approached **3a** both from the aromatic and the dithioles sides. The former interaction gives rise to a more stable association with a positive complexation (binding) energy of 8.98 kcal mol^{-1} (MPWB1K/6-31G** level).[21] The structure calculated for the resulting **3a**·C_{60} complex is shown

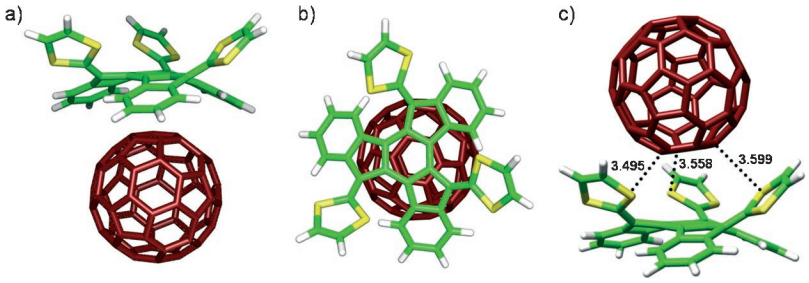

Figure 5. Structures of the **3a**·C_{60} complex calculated at the MPWB1K/6-31G** level. a) Side view of the preferred configuration. b) Top view of the same configuration, showing the stack between the central benzene ring of the truxene core and one of the hexagonal rings of C_{60}. c) Side view of the other possible configuration, with C_{60} approaching **3a** on the dithioles side. S–C short contacts [Å] are also shown. The carbon atoms of the fullerene are depicted in red for clarity.

in Figure 5a,b. The central benzene ring of the truxene core stacks on one of the benzene rings of C_{60} and leads to an almost parallel complex, in which the benzene rings are twisted by approximately 20° relative to each other and are located at an average distance of 3.39 Å. This distance is considerably shorter than that reported for the benzene dimer in parallel (3.9 Å) and parallel-displaced (3.6 Å) configurations.[22] In addition to the interactions of the central benzene ring, the peripheral benzene rings of **3a** show many intermolecular contacts in the 3.6–3.9 Å range with the C_{60} guest which contribute to stabilize the complex.

The interaction of C_{60} with the dithioles side of **3a** gives rise to the intermolecular complex depicted in Figure 5c for which a small binding energy of 2.28 kcal mol^{-1} is calculated. Theoretical calculations therefore suggest that the association of **3a** and C_{60} preferentially occurs on the aromatic face of **3a**, in agreement with experimental NMR evidence.

The association of C_{70} with **3a** was only studied by approaching C_{70} to the aromatic face of **3a**. Calculations converged to different minima of similar energy, depending on the relative orientation of **3a** and C_{70}. Among the minima localized, the two most stable configurations are those depicted in Figure S3 in the Supporting Information and have binding energies of 9.56 and 9.94 kcal mol^{-1}.

MPWB1K/6-31G** calculations therefore indicate that C_{70} interacts with **3a** more effectively than C_{60}, leading to slightly more stable complexes. MPWB1K/6-31 + G** calculations confirm this image (see the Supporting Information). Theoretical calculations are therefore in agreement with the higher value experimentally obtained for the association constant of the **3a**·C_{70} complex.

In conclusion, readily available truxene-TTFs **3** satisfactorily meet the requirements we proposed as necessary for the electron-donor partner to be used in the manufacture of fullerene-based self-assembled optoelectronic devices. The possibility of exploiting the elegant simplicity of the supramolecular **3a**–fullerene systems and the electronic and electrochemical properties of their components in the bottom-up construction of nanosized devices is currently under investigation. The potential application of the chiral properties of these compounds in the selective molecular recognition of inherently chiral higher fullerenes will also be investigated.

Received: October 23, 2006
Published online: January 24, 2007

Keywords: density functional calculations · fullerenes · π interactions · self-assembly · sulfur heterocycles

[1] a) J.-M. Lehn, *Science* **2002**, *295*, 2400–2403; b) T. Kato, N. Mizoshita, K. Kishimoto, *Angew. Chem.* **2006**, *118*, 44–74; *Angew. Chem. Int. Ed.* **2006**, *45*, 38–68.

[2] a) N. Martín, *Chem. Commun.* **2006**, 2093–2104; b) L. Sánchez, N. Martín, D. M. Guldi, *Angew. Chem.* **2005**, *117*, 5508–5516; *Angew. Chem. Int. Ed.* **2005**, *44*, 5374–5382; c) U. Hahn, M. Elhabiri, A. Trabolsi, H. Herschbach, A.-M. Albrecht-Gary, J.-F. Nierengarten, *Angew. Chem.* **2005**, *117*, 5472–5475; *Angew. Chem. Int. Ed.* **2005**, *44*, 5338–5341; d) D. M. Guldi, F. Zerbetto, V. Georgakilas, M. Prato, *Acc. Chem. Res.* **2005**, *38*, 38–43; e) O. Vostrowsky, A. Hirsch, *Angew. Chem.* **2004**, *116*, 2380–2383; *Angew. Chem. Int. Ed.* **2004**, *43*, 2326–2329; f) L. Echegoyen, L. E. Echegoyen, *Acc. Chem. Res.* **1998**, *31*, 593–601.

[3] T. Kawase, K. Tanaka, N. Shiono, Y. Seirai, M. Oda, *Angew. Chem.* **2004**, *116*, 1754–1756; *Angew. Chem. Int. Ed.* **2004**, *43*, 1722–1724.

[4] T. Yamaguchi, N. Ishii, K. Tashiro, T. Aida, *J. Am. Chem. Soc.* **2003**, *125*, 13934–13935.

[5] M. Shirakawa, N. Fujita, S. Shinkai, *J. Am. Chem. Soc.* **2003**, *125*, 9902–9903.

[6] J.-F. Nierengarten, U. Hahn, A. Trabolsi, H. Herschbach, F. Cardinali, M. Elhabiri, E. Leize, A. Van Dorsselaer, A.-M. Albrecht-Gary, *Chem. Eur. J.* **2006**, *12*, 3365–3373.

[7] For a recent review on concave–convex π–π interactions, see: T. Kawase, H. Kurata, *Chem. Rev.* **2006**, *106*, 5250–5273.

[8] For representative TTF–C_{60} conjugates, see: a) M. Segura, L. Sánchez, J. de Mendoza, N. Martín, D. M. Guldi, *J. Am. Chem. Soc.* **2003**, *125*, 15093–15100; b) N. Martín, L. Sánchez, M. A. Herranz, D. M. Guldi, *J. Phys. Chem. A* **2000**, *104*, 4648–4657.

[9] C. A. Christensen, A. S. Batsanov, M. R. Bryce, *J. Am. Chem. Soc.* **2006**, *128*, 10484–10490.

[10] For exTTF–C_{60} conjugates, see: a) L. Sánchez, M. Sierra, N. Martín, D. M. Guldi, M. W. Wienk, R. A. J. Janssen, *Org. Lett.* **2005**, *7*, 1691–1694; b) S. Handa, F. Giacalone, S. A. Haque, E. Palomares, N. Martín, J. R. Durrant, *Chem. Eur. J.* **2005**, *11*, 7440–7447; c) F. Giacalone, J. L. Segura, N. Martín, D. M. Guldi, *J. Am. Chem. Soc.* **2004**, *126*, 5340–5341.

[11] E. M. Pérez, L. Sánchez, G. Fernández, N. Martín, *J. Am. Chem. Soc.* **2006**, *128*, 7172–7173.

[12] a) Y. Sun, K. Xiao, Y. Liu, J. Wang, J. Pei, G. Yu, D. Zhu, *Adv. Funct. Mater.* **2005**, *15*, 818–822; b) A. L. Kanibolotsky, R. Berridge, P. J. Skabara, I. F. Perepichka, D. D. C. Bradley, M. Koeberg, *J. Am. Chem. Soc.* **2004**, *126*, 13695–13702; c) O. de Frutos, B. Gómez-Lor, T. Granier, M. A. Monge, E. Gutiérrez-Puebla, A. M. Echavarren, *Angew. Chem.* **1999**, *111*, 186–189; *Angew. Chem. Int. Ed.* **1999**, *38*, 204–207; d) for the synthesis and self-association studies of planar alkylated truxenes, see: O. de Frutos, T. Granier, B. Gómez-Lor, J. Jiménez-Barbero, M. A. Monge, E. Gutiérrez-Puebla, A. M. Echavarren, *Chem. Eur. J.* **2002**, *8*, 2879–2890.

[13] A. J. Moore, M. R. Bryce, *Synthesis* **1991**, 26–31.

[14] Crystal data for **3a**·2 $CHCl_3$: $C_{38}H_{20}Cl_6S_6$, $M_r = 881.60$, red prismatic ($0.06 \times 0.16 \times 0.32$ mm^3), monoclinic, space group C2/c, $a = 34.049(2)$ Å, $b = 11.3457(8)$ Å, $c = 19.970(1)$ Å, $\beta = 105.387(1)°$, $V = 7438.0(9)$ Å^3, $Z = 8$, $\rho_{calcd} = 1.575$ g cm^{-3}, $F(000) = 3568$, $\mu = 0.829$ mm^{-1}, $2\theta_{max} = 50.0°$, $T = 296(2)$ K, 6565 unique reflections [$R_{int} = 0.116$], $R1 = 0.073$, $wR2 = 0.2353$ (all data). GOF(F^2) = 1.091, $N_0/N_V = 6565/439$, highest residual electron density 1.273 e Å^{-3}. X-ray diffraction data were measured on a Bruker Smart CCD diffractometer, with graphite-monochromated $Mo_{K\alpha}$ radiation ($\lambda = 0.71073$ Å). The structure was solved by direct methods. The refinement was done by full-matrix least-squares procedures on F^2 (SHELXTL version 5.1). Non-hydrogen atoms were refined anisotropically. All hydrogen atoms were calculated at their geometrical positions and refined as riding on their respective carbon atoms. CCDC 623710 contains the supplementary crystallographic data for this paper. These data can be obtained free of charge from The Cambridge Crystallographic Data Centre via www.ccdc.cam.ac.uk/data_request/cif.

[15] S. Amriou, C. Wang, A. S. Batsanov, M. R. Bryce, D. F. Perepichka, E. Ortí, R. Viruela, J. Vidal-Gancedo, C. Rovira, *Chem. Eur. J.* **2006**, *12*, 3389–3400.

[16] *Electrochemical Methods. Fundamentals and Applications* (Eds.: A. J. Bard, L. R. Faulkner), Wiley, New York, **2001**.

[17] N. Martín, E. Ortí, L. Sánchez, P. M. Viruela, R. Viruela, *Eur. J. Org. Chem.* **1999**, 1239 – 1247.
[18] The 1:1 stoichiometry was further confirmed by Job plot analysis. See Figure S4 in the Supporting Information.
[19] Y. Zhao, D. G. Truhlar, *Phys. Chem. Chem. Phys.* **2005**, *7*, 2701 – 2705.
[20] The B3LYP functional does not account for stacking interactions because it fails badly for dispersion interactions. See: a) S. Tsuzuki, H. P. J. Luthi, *Chem. Phys.* **2001**, *114*, 3949 – 3957; b) Y. Zhao, D. G. J. Truhlar, *Chem. Theory Comput.* **2005**, *1*, 415 – 432.
[21] Complexation binding energies are calculated as the difference between the sum of the total energies of **3a** and C_{60} and the total energy of the **3a**·C_{60} complex.
[22] a) T. Sato, T. Tsuneda, K. J. Hirao, *Chem. Phys.* **2005**, *123*, 104307; b) M. O. Sinnokrot, C. D. Sherrill, *J. Phys. Chem. A* **2004**, *108*, 10200 – 10207; c) M. O. Sinnokrot, E. F. Valeev, C. D. Sherrill, *J. Am. Chem. Soc.* **2002**, *124*, 10887 – 10893.

